Supporting Information

Preparation of Near-infrared Photoacoustic Imaging and Photothermal Treatment Agent for Cancer Using a Modifiable Acid-triggered Molecular Platform

Xiaoming Liu, ‡ [a, b, c] Chunbai Xiang, ‡ [b,c] Yalin Lv, ‡ [b, c] Jingjing Xiang, [b, c] Gongcheng Ma [b,c] , Changzhong Li [d], Yan Hu [d], Chunlei Guo [d], Hua Sun[*a] Lintao Cai [*b, c] and Ping Gong, [*b,c]

a. College of Bioengineering, Tianjin University of Science and Technology, Tianjin 300222, China. *E-mail: sunhua@tust.edu.cn

b. Guangdong Key Laboratory of Nanomedicine, CAS Key Laboratory of Health Informatics, Shenzhen Bioactive Materials Engineering Lab for Medicine, Institute of Biomedicine and Biotechnology, Shenzhen Institute of Advanced Technology, Chinese Academy of Sciences, Shenzhen 518055, China. *E-mail: ping.gong@siat.ac.cn.

c. Sino-Euro Center of Biomedicine and Health, Luohu Shenzhen 518024, China.

d. Peking University Shenzhen Hospital, Shenzhen, 518053, China

Experimental section

General Information of Materials and Methods

N,N-Dimethylformamide (DMF), dichloromethane, methanol, triethylamine (TEA), 4-dimethylaminopyridine (DMAP), and other chemical reagents were purchased from J&K Scientific. DMEM medium, fetal bovine serum (FBS), and kanamycin sulfate were purchased from Invitrogen Co. Ltd. All reagents were purchased from commercial suppliers and used without further purification. The solvents used were purified by standard methods before use. MCF-7 cells were kindly provided by the Cell Center of our institute. The buffer solutions were as follows: the high K^+ buffer containing 30 mM NaCl, 120 mM KCl, 1 mM $CaCl_2$, 0.5 mM $MgSO_4$, 1 mM NaH_2PO_4, 5 mM glucose, 20 mM HEPES (various pH values were adjusted using NaOH); phosphate buffered saline solution (PBS) containing 137 mM NaCl, 2.7 mM KCl, 4.3 mM NaH_2PO4, 1.4 mM KH_2PO4 (pH 7.4). 1H NMR spectra were recorded on CDCl3 solutions using a Bruker AM-400 spectrometer. Mass spectra were obtained using a JMS-HX 110A / 110A Tandem Mass Spectrometer (JEOL). Deionized water was used to prepare all aqueous solutions.

Synthesis of Compound IR-PZ

IR755 (34.4 mg, 0.4 mmol) was dissolved in anhydrous DMF (2 mL), and piperazine (63.8 mg, 0.1 mmol) was added. The mixture was stirred at 80 °C for 1h under Nitrogen atmosphere. Finally, the solvent was evaporated under reduced pressure to give the crude product, which was further purified by silica gel column chromatography with dichloromethane and methanol to afford pure blue product. Yield: 55 mg (80%). ^{1}H NMR (400 MHz, $CDCl_3$) δ 7.86 (d, J = 13.6 Hz, 2H), 7.48 (d, J = 7.3 Hz, 2H), 7.37 (t, J = 7.7 Hz, 2H), 7.22 (t, J = 7.4 Hz, 2H), 7.04 (d, J = 7.9 Hz, 2H), 5.89 (d, J = 13.6
Hz, 2H), 4.20 (s, 4H), 4.06 (q, J = 7.2 Hz, 4H), 3.63 (t, J = 5.1 Hz, 4H), 2.52 (t, J = 6.4 Hz, 4H), 1.90 (s, 2H), 1.85 (s, 12H), 1.45 (t, J = 7.2 Hz, 6H). HRMS (ESI+): m/z $C_{38}H_{49}N_4^+$calcd. 561.3952, found [M^+]
561.3946.

Synthesis of Compound IR-PE

IR-PZ (34.4 mg, 0.05 mmol) was dissolved in anhydrous DMF (2 mL), and iodoethane (39 mg, 0.25 mmol), triethylamine (TEA) (35 μL, 0.25 mmol) was added. The mixture was stirred at 60 °C for 2h under Nitrogen atmosphere. Finally, the solvent was evaporated under reduced pressure to give crude products, which were further purified by silica gel column chromatography with dichloromethane and methanol to afford the pure blue product. Yield: 23 mg (65%).^{1}H NMR (400 MHz, $CDCl_3$) δ 7.71 (d, J = 13.5 Hz, 2H), 7.42 (d, J = 7.3 Hz, 2H), 7.34 (t, J = 7.4 Hz, 2H), 7.18 (t, J =
7.4 Hz, 2H), 7.00 (d, J = 7.9 Hz, 2H), 5.84 (d, J = 13.5 Hz, 2H), 4.07 – 3.58 (m, 14H), 2.49 (t, J = 6.4
Hz, 4H), 1.86 (dt, J = 13.3, 6.7 Hz, 2H), 1.80 (s, 12H), 1.66 (t, J = 7.2 Hz, 3H), 1.42 (t, J = 7.2 Hz, 6H). HRMS (ESI+): m/z$C_{40}H_{53}N_4^+$ calcd. 561.3952, found [M^+] 561.3952.

Synthesis of Compound IR-PZM

IR-PZ (34.4 mg, 0.05 mmol) was dissolved in anhydrous DMF (2 mL), and 4-(bromomethyl) pyridine hydrobromide (50.6 mg, 0.4 mmol), triethylamine (TEA) (70 μL, 0.5 mmol) was added. The mixture was stirred at 60 °C for 2h under Nitrogen atmosphere. Finally, the solvent was evaporated under reduced pressure to give the crude products, which were further purified by silica gel column chromatography with dichloromethane and methanol to afford the pure blue product. Yield: 58 mg (60%).^{1}H NMR (400 MHz, $CDCl_3$) δ 8.77 (s, 1H), 8.62 (s, 1H), 8.11 (d, J = 6.9 Hz, 1H), 7.67 (d, J =
13.4 Hz, 2H), 7.47 – 7.41 (m, 1H), 7.35 (dd, J = 15.9, 7.7 Hz, 4H), 7.17 (t, J = 7.4 Hz, 2H), 7.00 (d, J =
7.9 Hz, 2H), 5.83 (d, J = 13.4 Hz, 2H), 4.13 – 3.80 (m, 10H), 3.02 (s, 4H), 2.50 (t, J = 6.5 Hz, 4H), 1.89 – 1.81 (m, 2H), 1.69 (s, 12H), 1.40 (t, J = 7.2 Hz, 6H). HRMS (ESI+): m/z$C_{44}H_{54}N_5^+$calcd. 652.4374, found [M^+] 652.4376.

Synthesis of Compound IR-PEA

First,2-bromoethan-1-amine (1.02 g, 5 mmol), 1-(9-fluorenyl) methyl chloroformate (1.05 g, 4.05 mmol) was dissolved in 15 mL 1,4-dioxane, and sodium bicarbonate (2 eq) was added slowly with stirring. The resulting mixture was stirred at room temperature overnight. 10 ml H_2O was then added and the mixture was extracted 3 times with ethyl acetate. The ethyl acetate phase was

evaporated under reduced pressure to give a crude white solid. The white solid (41 mg, 0.2 mmol), IR-PZ (34.4 mg, 0.05 mmol), and triethylamine (14 μL, 0.1 mmol) were dissolved in anhydrous DMF (2 mL). The mixture was stirred at 40 °C for 4h under Nitrogen atmosphere. Finally, the solvent was evaporated under reduced pressure to give the crude product, which was further purified by silica gel column chromatography with dichloromethane and methanol to afford a pure blue product. Yield: 15 mg (42%).1H NMR (400 MHz, $CDCl_3$) δ 7.63 (d, J = 13.0 Hz, 2H), 7.37 (d, J = 7.2 Hz, 2H),
7.30 (t, J = 7.6 Hz, 2H), 7.11 (t, J = 7.3 Hz, 2H), 6.94 (d, J = 7.8 Hz, 2H), 5.71 (d, J = 13.1 Hz, 2H), 4.78-
4.70 (m, 2H), 4.08 – 3.79 (m, 10H), 3.52-3.43 (m, 2H), 3.14-3.05 (m, 4H), 2.45 (t, J = 6.1 Hz, 4H),
1.81 (dd, J = 14.7, 8.4 Hz, 2H), 1.69 (s, 12H), 1.38 (t, J = 6.9 Hz, 6H). HRMS (ESI+): m/z $C_{40}H_{54}N_4^+$calcd.
604.4374, found [M^+] 604.4375.

Synthesis of Compound IR-PHA

IR-PZ (34.4 mg, 0.05mmol) was dissolved in anhydrous DMF (2 mL), and 6-Bromohexanoic acid (39 mg, 0.2 mmol), triethylamine (TEA) (70 μL, 0.5 mmol) was added. The mixture was stirred at 60 °C for 4 h under Nitrogen atmosphere. Finally, the solvent was evaporated under reduced pressure to give the crude products, which were further purified by silica gel column chromatography with dichloromethane and methanol to afford the pure blue product. Yield: 13 mg (40%).^{1}H NMR (400 MHz, $CDCl_3$) δ 7.67 (d, J = 13.4 Hz, 2H), 7.38 (d, J = 7.3 Hz, 2H), 7.33 (t, J = 7.7 Hz, 2H), 7.15 (t, J =
7.4 Hz, 2H), 6.99 (d, J = 7.9 Hz, 2H), 5.80 (d, J = 13.4 Hz, 2H), 4.05 – 3.87 (m, 8H), 3.08 (m, 4H), 2.84
(m, 2H), 2.54 – 2.42 (m, 6H), 1.88 – 1.80 (m, 2H), 1.79 – 1.72 (m, 4H), 1.70 (s, 12H), 1.54 – 1.48 (m, 2H), 1.40 (t, J = 7.2 Hz, 6H). HRMS (ESI+): m/z$C_{44}H_{59}N_4O_4^+$, calcd. 675.4633, found [M^+] 604.4633.

Optical Properties Measurement

Absorption spectra of probes were obtained in 0.1 M sodium phosphate buffer with different pH values containing 10% (v/v) DMSO as a cosolvent, using a PerkinElmer Lambda 25 UV-vis spectrophotometer (PerkinElmer Co., USA). The fluorescence spectra were investigated on an FSP920 spectrofluorometer (Edinburgh Instruments Ltd., United Kingdom). The excitation and emission monochromator slits were both set to 2 nm, 3 nm, respectively. For determination of the quantum efficiency (Q.E.) of fluorescence, cresyl violet in methanol (Q.E. = 0.54) was used as a standard. Values were calculated according to the reference.

Cell culture

Cells were cultured in 1640 medium containing 10% fetal bovine serum (FBS), 100 U/mL penicillin, and 100 μg/ml streptomycin in a humidified atmosphere with 5% CO_2 at 37 °C. The cells were maintained in an exponential growth phase by periodic subcultivation. The cell density was determined using a hemocytometer, and this was performed before any experiments.

In vitro cell uptake

MCF-7 cells (1×10^4) were seeded into 8-well chambered cover glasses (Lab-Tek, Nunc, USA) in 200 μL of medium, respectively. After 24 h, 10 μg/mL probe was incubated with cells for 4 h at 37 °C. The cells were washed thrice with PBS. The nuclear dye hochest 33258 was used as a positive control to stain nuclei in the experiment. Finally, the fixed cells were observed by a confocal laser scanning microscope (Leica TCS SP5, GER).
For the cellular uptake experiment, the cells (1×10^5 cells per well) were seeded in 6-well plates and incubated overnight, and then incubated with 5 μg/mL probe. After incubation for 4 h, cells were rinsed with PBS three times, trypsinized, and resuspended with medium. Afterward, the cells were collected by FACSCantoTM II Gallios flow cytometer (BD Biosciences) and analyzed by CFlow Plus software (BD, Ann Arbor, MI).

In vitro photothermal efficiency

1 mL of PBS, IR-PHA (20 mg/ml) was added into different wells of 24-wellplate. Using 1.6 W/cm^2 laser to irradiate the 5 samples for 8 min simultaneously, the temperature changes of each group were recorded by an infrared thermal imaging camera (Ti27, Fluke, USA).

Animals and tumor model

50 BALB/c nude mice were provided by the Medical Experimental Animal Center of Guangdong Province. They were 4-6 weeks old at the start of each experiment and weighed 20-25 g. For tumor implantation, 30 nude mice received a subcutaneous injection of 5×10^6 MCF-7 cells suspended in
0.2 mL of saline solution in the left hind limb. Tumors were then allowed to grow to 1-2 cm in diameter for 10–30 days. All animal operations were in according with institutional animal use and care regulations, approved by the Laboratory Animal Center of Guangdong.

PA imaging

The photoacoustic imaging (PA) of mice was performed with a Nexus 128 small animal photoacoustic 3-D tomographic imaging system (Endra Life Sciences, USA). The PA images were captured at 680 nm and 760 nm. The I_{760}/I_{680} ratios calculated by the software of the PA imaging system could be used to measure the pH value. For in vivo imaging, each mouse was injected with a 100 μl 0.16 mg/mL probe intravenously.

Fluorescence imaging

The NIR-Ia imaging was obtained by using the Xenogen Caliper spectrum IVIS system (Xenogen, USA) equipped with a Si CCD camera. The excitation wavelength was from 655-685 nm and 730- 760, respectively. A bandpass filter from 790-810 nm was selected as an emission passband.

In vivo tumor photothermal treatment

Tumor-bearing models were made as described by animals and tumor models. Four groups of mice were prepared and divided into PBS, PBS + laser, probe, and probe + laser group. When the tumor grew to 50 mm^3 in volume. 150 μl of IR-PHA solution (200 μg/mL) was injected into mice via the tail vein. After 24 h, the groups of PBS+laser, and probe+laser, were irradiated with 808nm laser (0.8 W/cm^2, 5 min). During the 40 days, the weight, and tumor volumes of mice were monitored. Tumor volume = (tumor length) × (tumor width) $^2/2$. Mice with tumor volumes exceeding 600 cm^3 would be euthanatized according to animal protocol, and the slow growth and malignance of this tumor model.

Statistical Analysis

Data were reported as mean ±SD. The differences among groups were determined using one-way ANOVA analysis followed by Tukey's post-test (*) $P < 0.05$, (**) $P < 0.01$.

Theoretical Calculation[1,2]

All theoretical calculations in this article were completed in Gaussian 16, using the IEFPCM
solvation model to simulate the water environment. DFT and TD-DFT methods were used based on B3LYP/6-311G (d, p) to optimize the specific calculation of ground state (S_0) and vertical excitation energy for the five diagnostic and therapeutic probes, as well as the geometric structure optimization of the excited state (S_1). Frequency calculations were also performed, and the imaginary frequencies were all zero, ensuring that each electronic state was located at the local energy minimum point. To better describe the dispersion effect, we introduced the D3 correction method with Becke Johnson damping in all calculation processes. All molecular frontier orbitals in the article, as well as the Root mean square displacement (RMSD) of the ground state (S_0) and excited state (S_1) structures of the probes before and after protonation, were analyzed using the wave function software Multiwfn and VMD visualization software developed by Lu Tian et al. The non-radiative transition rate (K_{ic}), recombination energy (RE), and Huang-Rhys factor (HR) were calculated using FCClass3.0 combined with Gaussian 16 to calculate the ground state and excited state. The vibration vector of the probe was obtained from a Gaussian View.[1,2]

Figures and tables

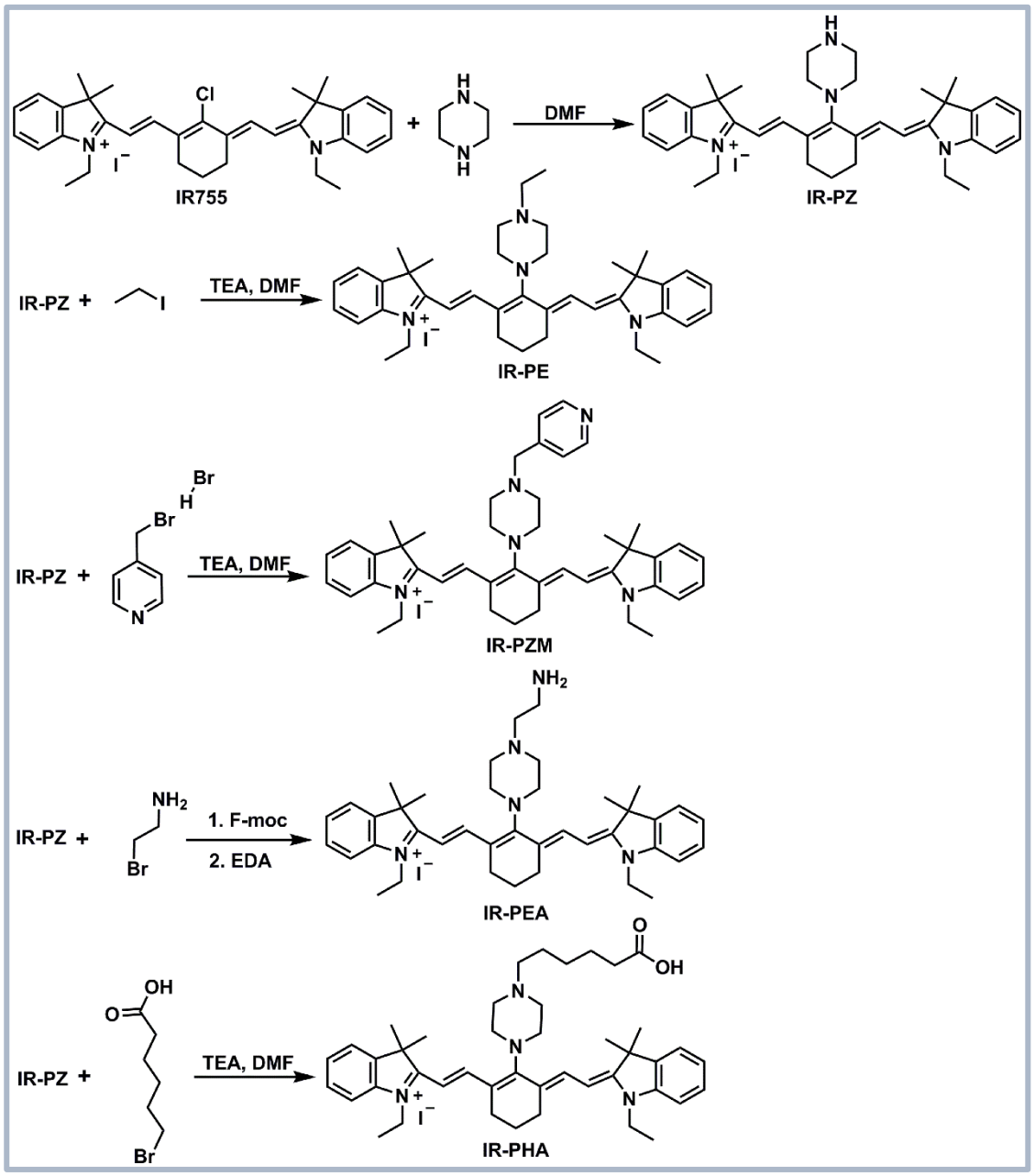

Fig S1. Synthesis scheme for IR-PZ derivatives

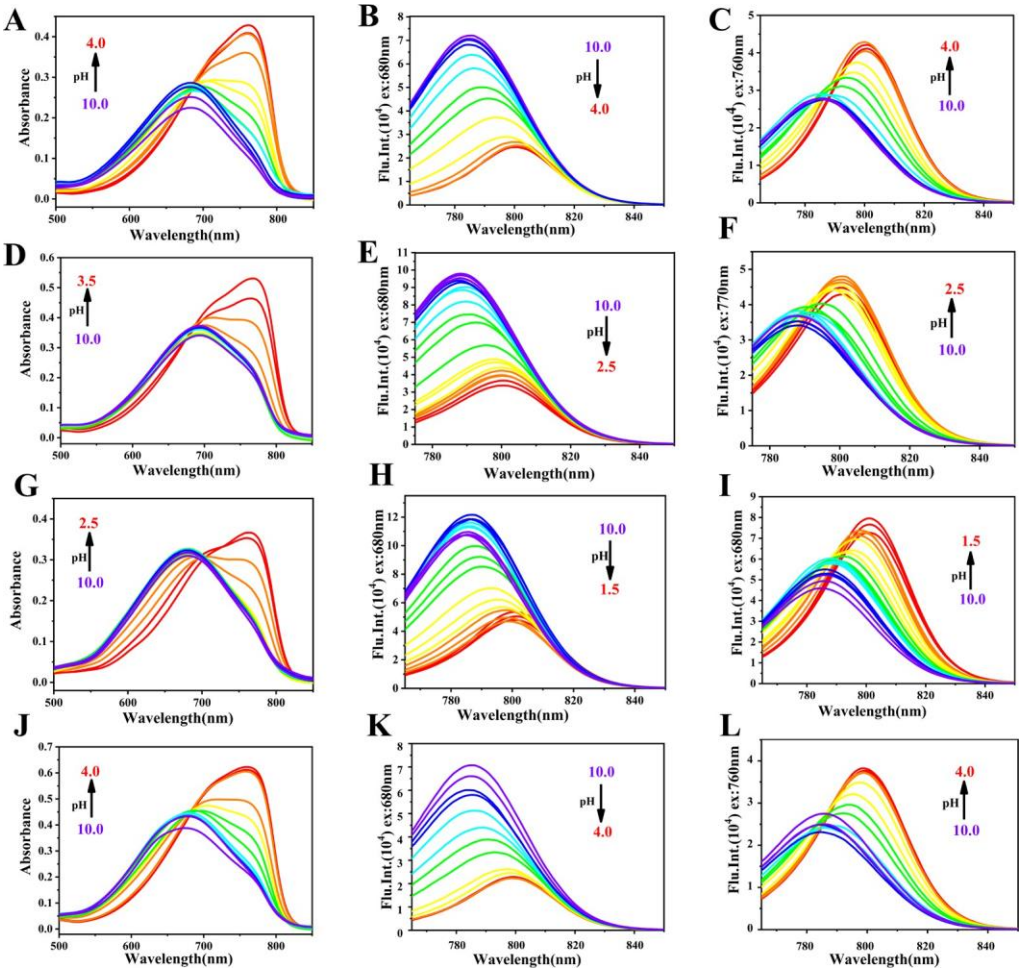

Figure S2. Absorption spectrum of (A) IR-PE, (D) IR-PZM, (G)IR-PEA, (J) IR-PHA in buffer/DMSO solution (v/v = 9:1) with 8 μM. PL spectrum of (B) IR-PE, (E) IR-PZM, (H) IR-PEA, (K) IR-PHA in buffer/DMSO solution (v/v = 9: 1) with 8 μM (λ_{ex} = 680 nm). PL spectrum of (C) IR-PE, (F) IR-PZM,
(I) IR-PEA, (L) IR-PHA in buffer/DMSO solution (v/v = 9:1) with 8 μM (λ_{ex} = 760 nm).

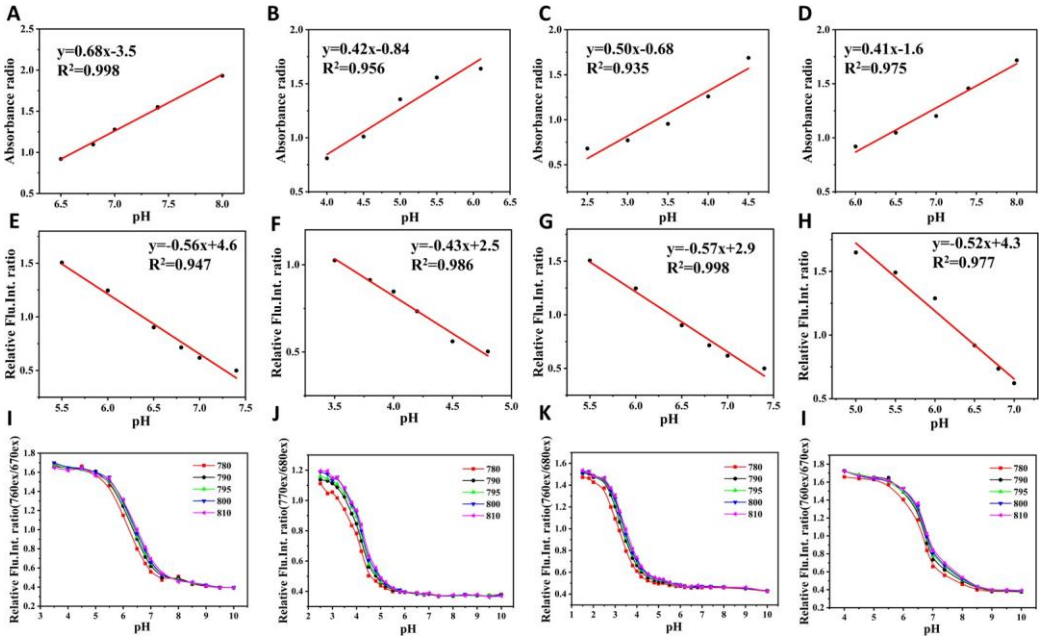

Figure S3. Linear relationship of absorbance ratio of (A) IR-PE, (B) IR-PZM, (C) IR-PEA, and (D) IR- PHA against pH value is observed over the range of pH 6.5-8.0, 4.0-6.5, 2.5-4.5, 6.0-8.0. Linear relationship of the fluorescence intensity ratio of (E) IR-PE, (F) IR-PZM, (G) IR-PEA, and (H) IR-PHA against pH value is observed over the range of pH 5.5-7.5, 3.5-4.8, 2.5-3.8, 5.0-7.0. Relative fluorescence intensity ratio of (I) IR-PE, (J) IR-PZM, (k) IR-PEA, and (l) IR-PHA at various pH values (λ_{ex} = 760 nm/λ_{ex} = 680 nm, λ = 780, 790, 795, 800, 810 nm).

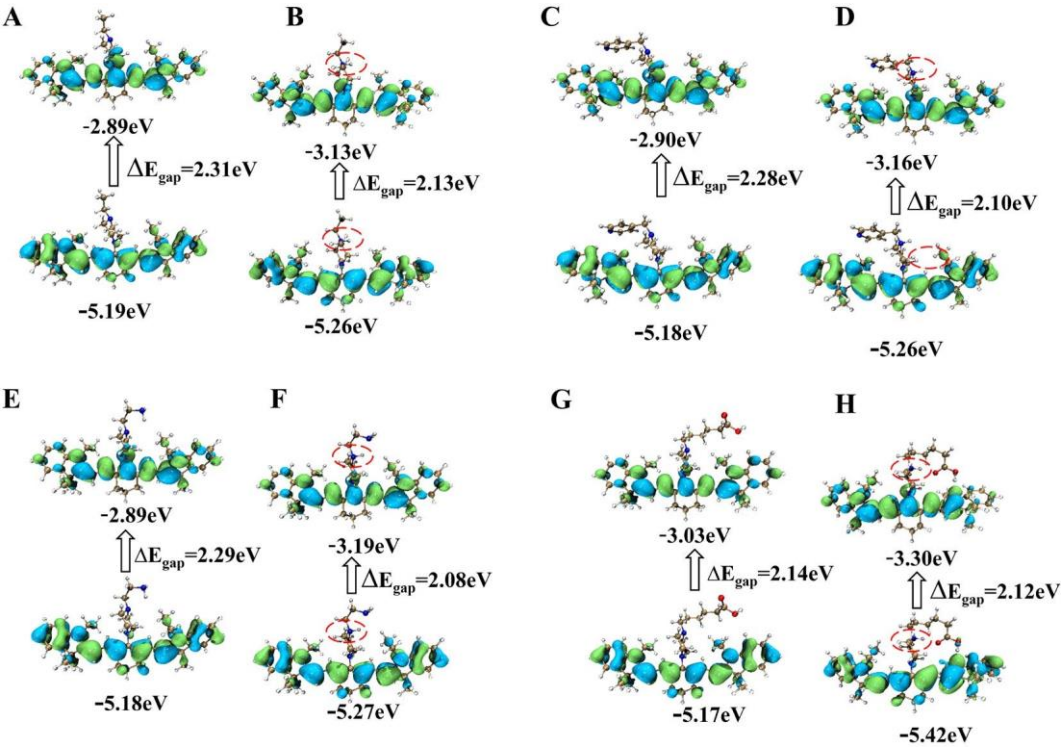

Figure S4. HOMO–LUMO distribution of (A) IR-PE, (B) IR-PE/H^+, (C) IR-PZM, (D) IR-PZM/H^+,

(E) IR-

PEA, (F) IR-PEA/H^+, (G) IR-PHA, (H) IR-PHA/H^+.

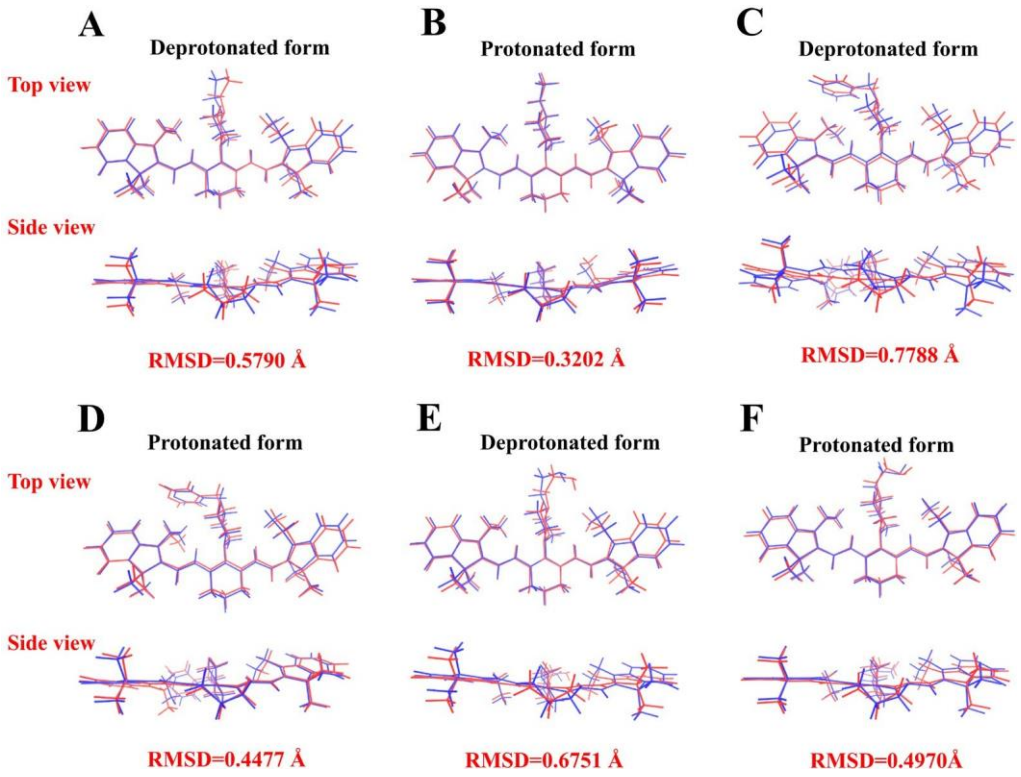

Figure S5. Minimum energy geometries of (A) IR-PE, (B) IR-PE/H^+, (C) IR-PZM, (D) IR-PZM/H^+ (E) IR- PEA and (F) IR-PEA/H^+ was calculated for the S_0 (blue) and S_1 (red) electronics states.

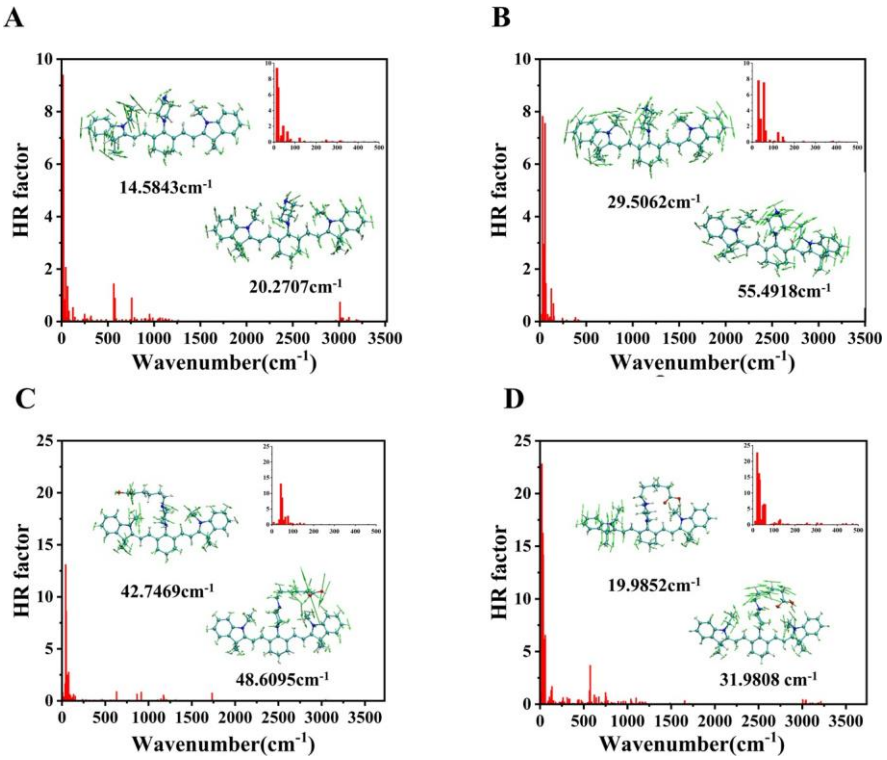

Figure S6. HR factor of (A)IR-PZ, (B) IR-PZ/H^+, (C) IR-PHA and (D) IR-PHA/H^+. Inset: the top two vibration vectors of HR factor.

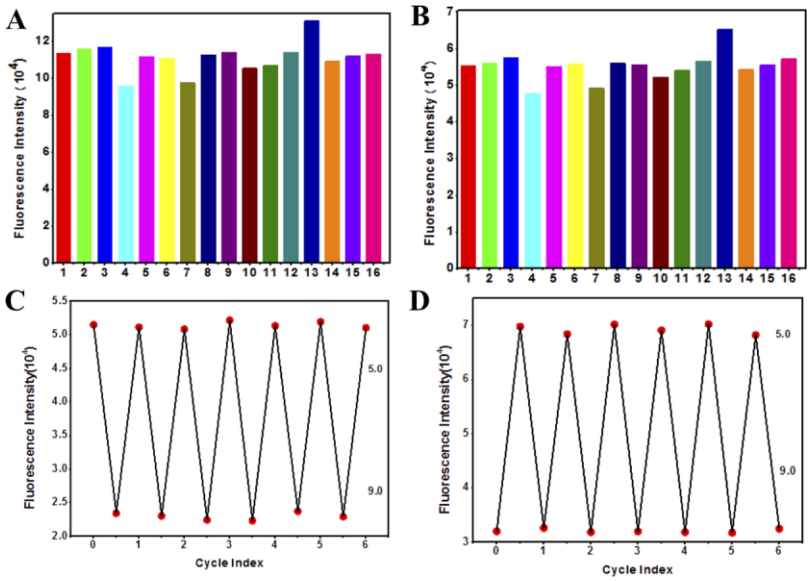

Figure S7. Ion selectivity of IR-PHA under different excitation conditions. (A) λ_{ex} = 680 n m; (B) λ_{ex} = 760 nm. (1.IR-PHA; 2-16(0.5mM): K^+, Na^+, Ca^{2+}, Fe^{2+}, Fe^{3+}, Cu^{2+}, Zn^{2+}, Mg^{2+},
Ag^+, Cd^{2+}, Co^{2+}, Mn^{2+}, Ni^{2+}, Pb^{2+}, Sn^{2+}.) pH reversibility of IR-PHA between pH 5.0 and 9.
0. (C) λ_{ex} = 680 nm; (D) λ_{ex} = 760 nm.

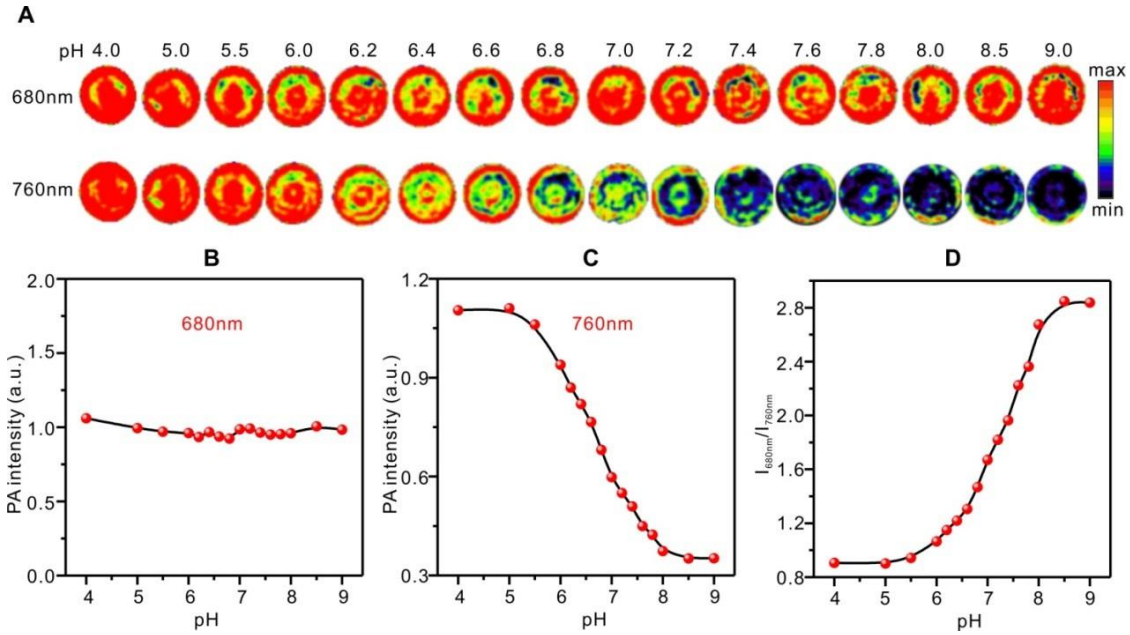

Figure S8. Photoacoustic imaging of IR-PHA at absorption wavelengths of 680 nm and 760 nm in different pH solutions.

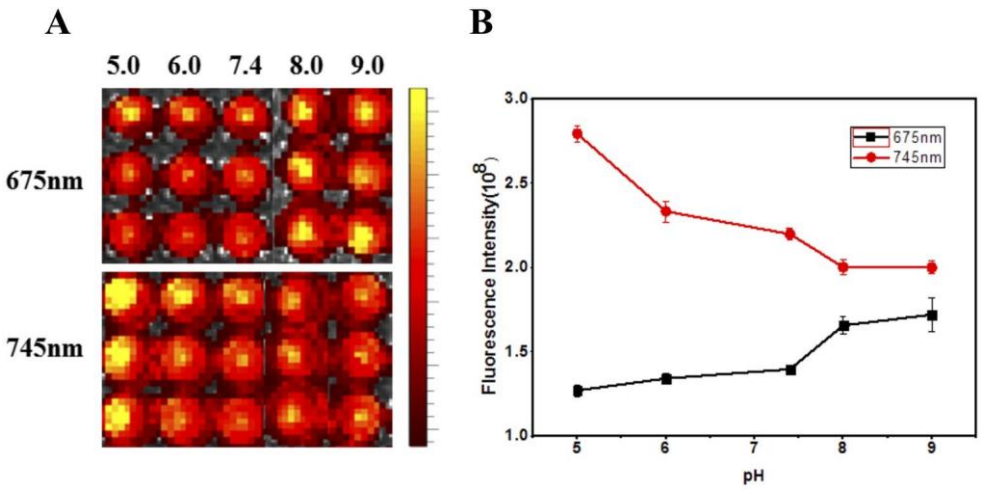

Figure S9. IR-PHA fluorescence imaging in different excitation wavelengths and different pH solutions.

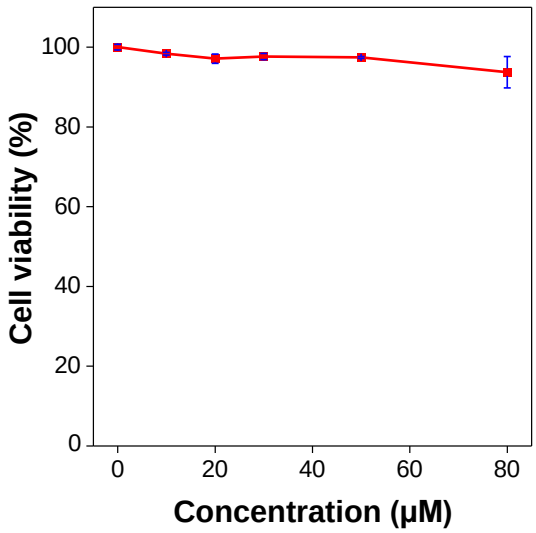

Figure S10. Cytoviability of MCF-7 cells breast cancer cells after incubation with different concentrations of IR-PHA for 24 h.

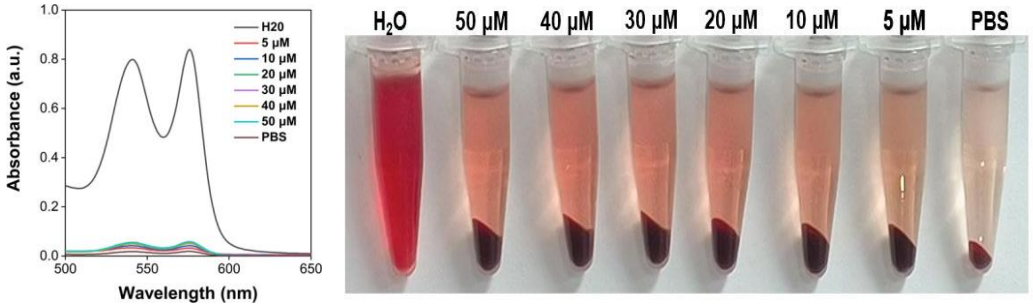

Figure S11. The hemolysis assays of IR-PHA.

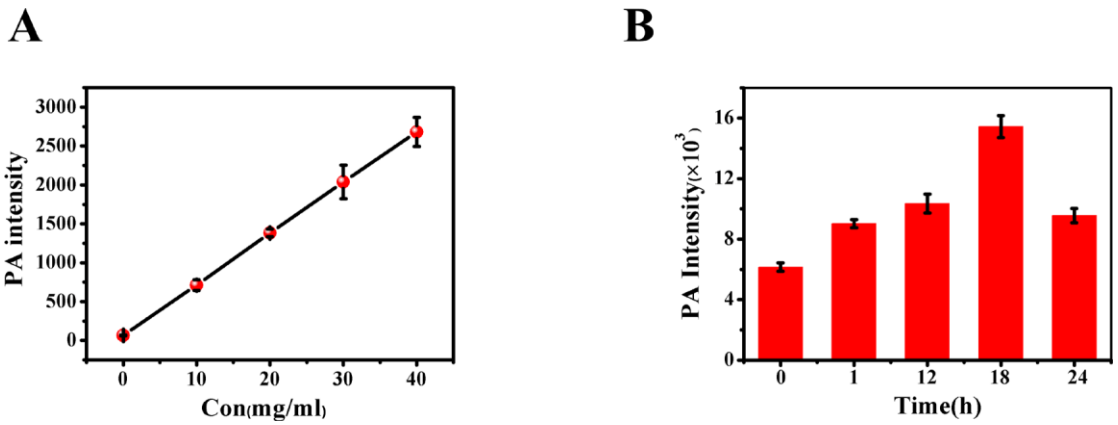

Figure S12. (A) The linear fitting of the relative PA intensity and the concentration of IR-PHA (0-40 mg /mL). (B)The quantitatively analyzed of the Photoacoustic images of the vascular tissue around the tumor tissue at selected times (0, 1, 12, 18, 24 h) post-incubation of IR-PHA (40 mg/mL).

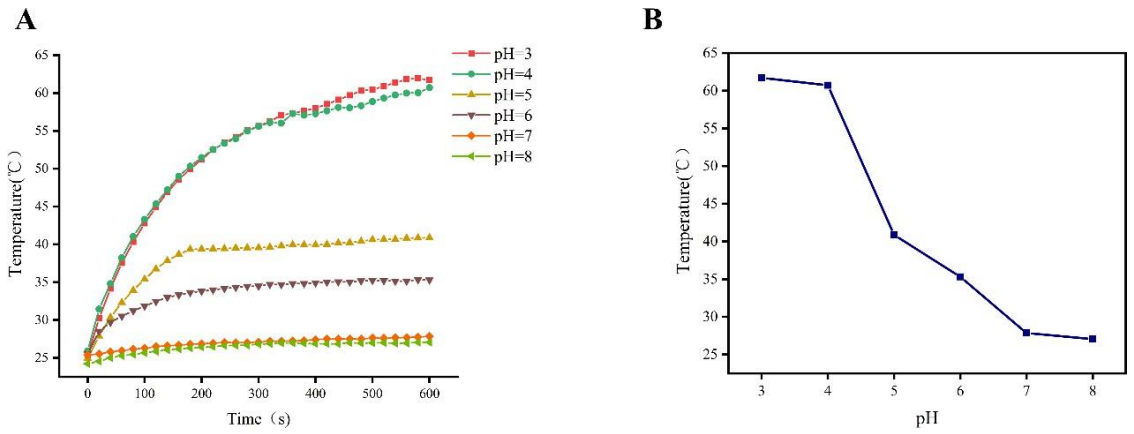

Figure S13. (A) pH-dependent temperature increase profiles of IR-PHA (40ug/ mL1) as a function of laser irradiation time (808 nm, 1W/ cm^2). (B) The highest temperature can be reached at the corresponding pH.

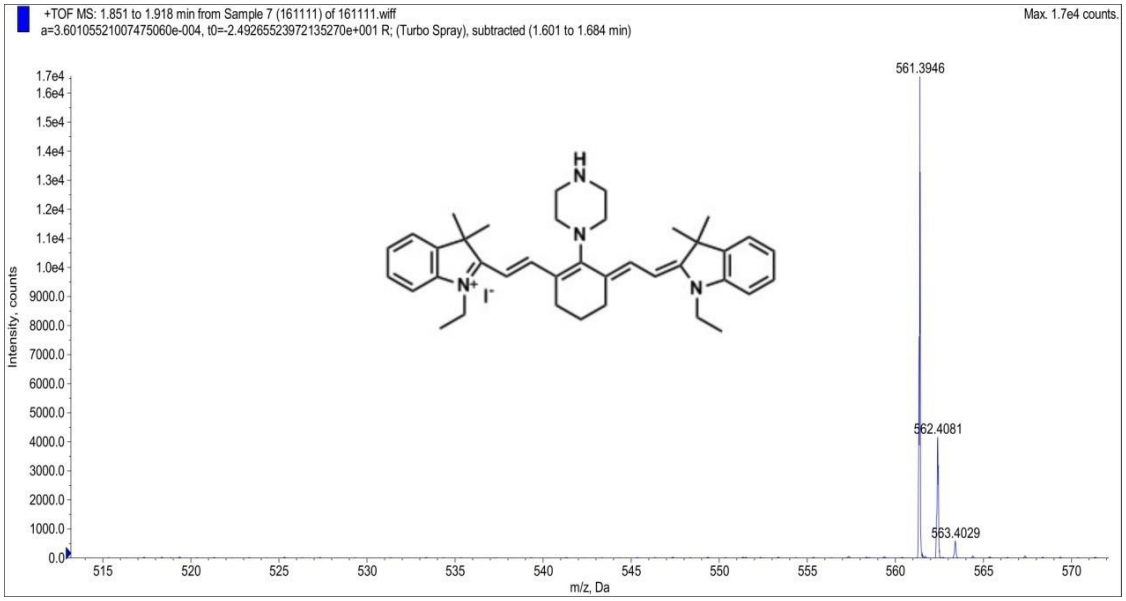

Figure S13. High resolution mass spectrometry (HRMS) of IR-PZ

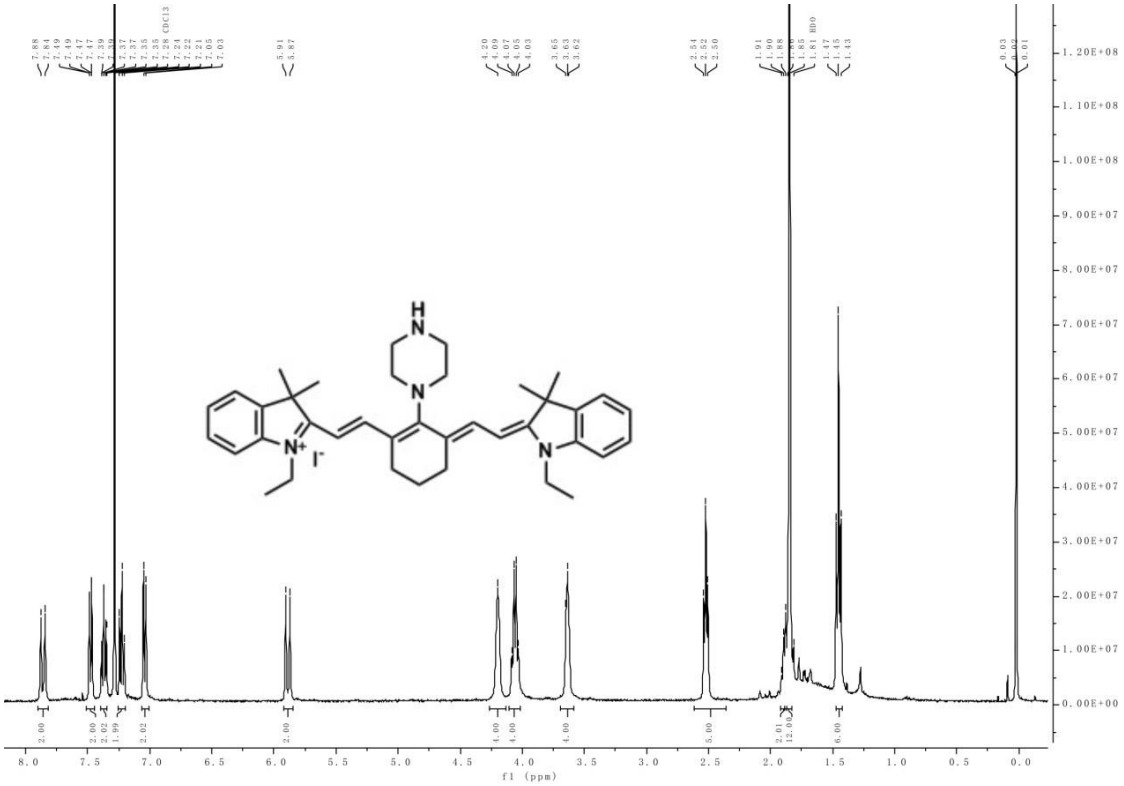

Figure S14. ^{1}H NMR Spectrum of IR-PZ in $CDCl_3$

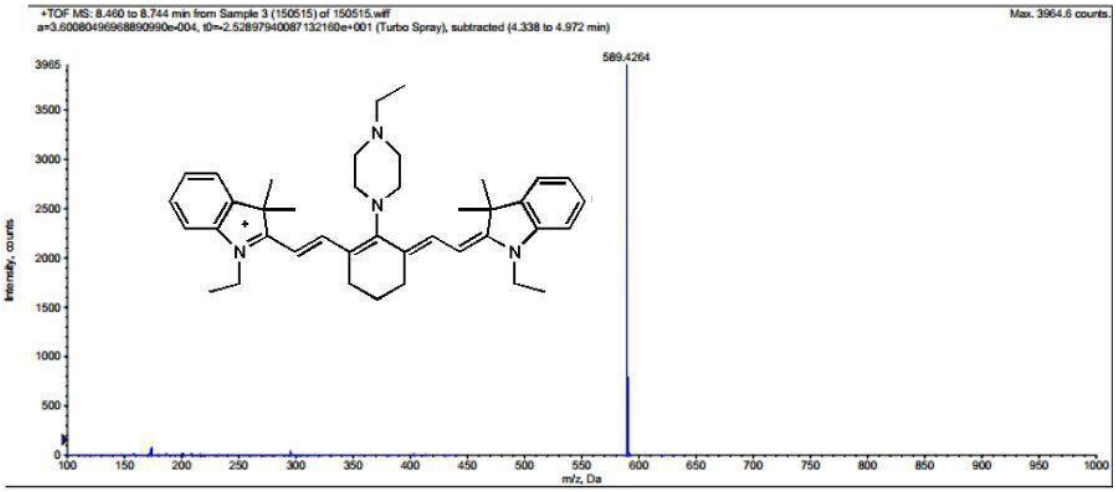

Figure S15. High resolution mass spectrometry (HRMS) of IR-PE

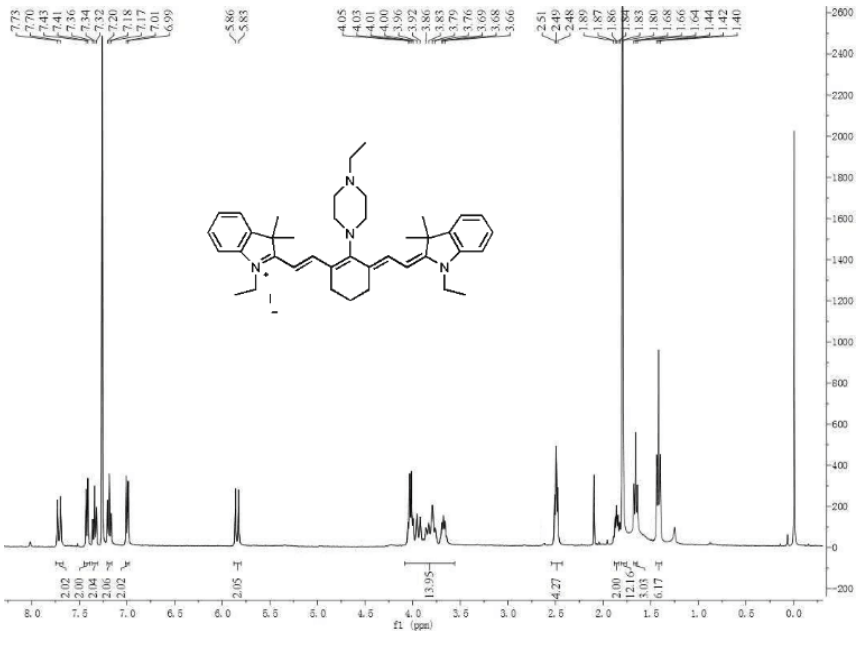

Figure S16. ^{1}H NMR Spectrum of IR-PE in $CDCl_3$

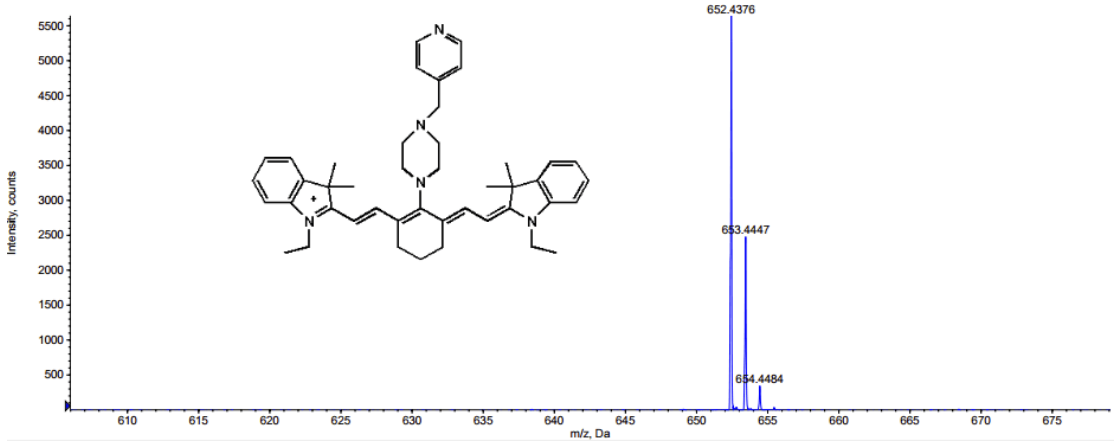

Figure S17. High resolution mass spectrometry (HRMS) of IR-PZM

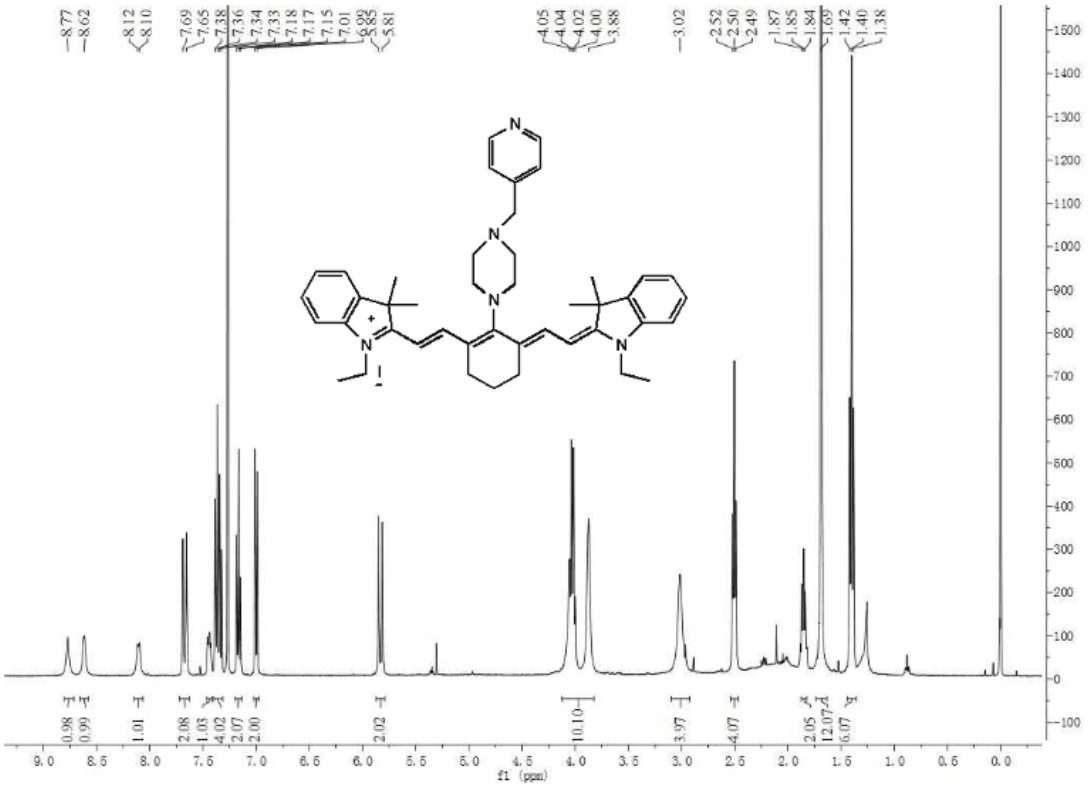

Figure S18. ^{1}H NMR Spectrum of IR-PZM in $CDCl_3$

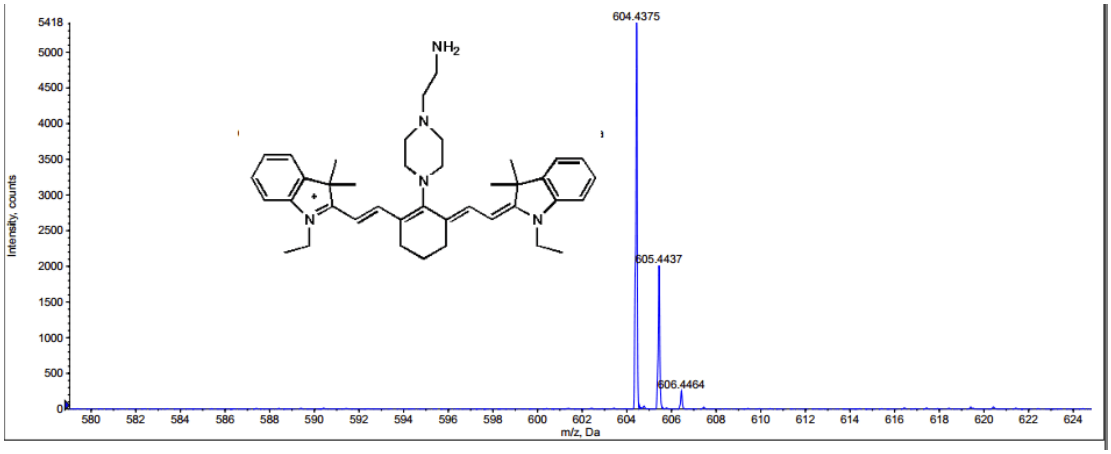

Figure S19. High resolution mass spectrometry (HRMS) of IR-PEA

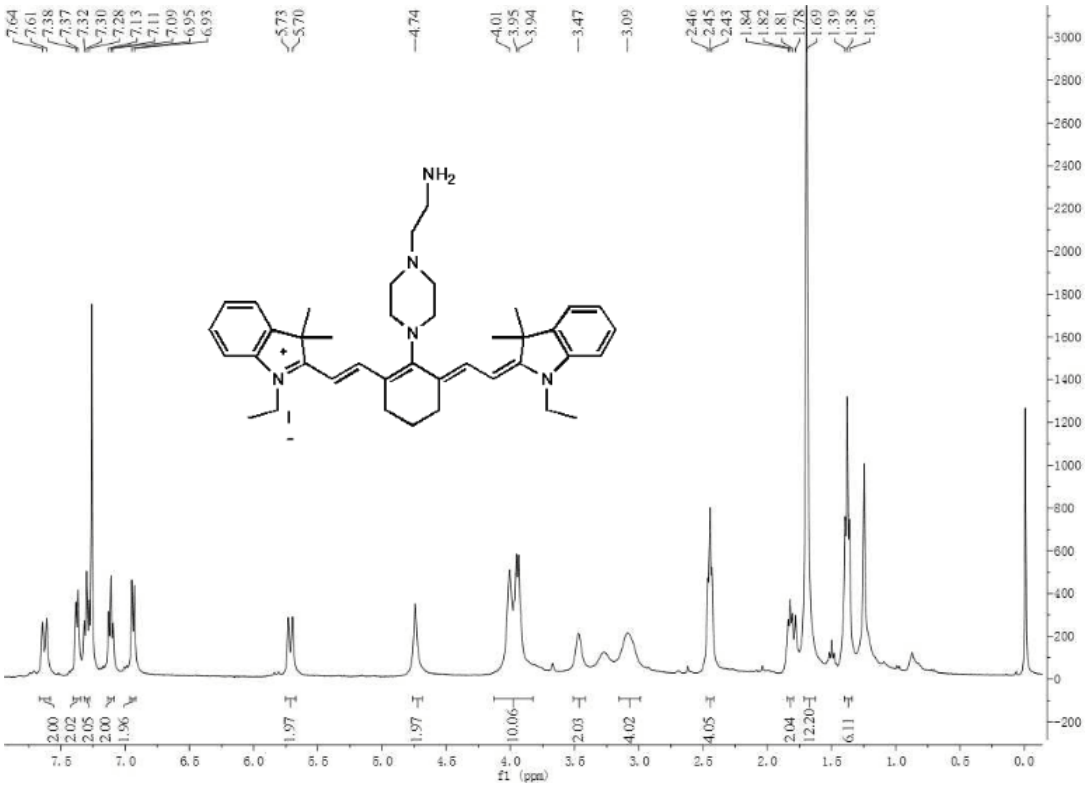

Figure S20. ^{1}H NMR Spectrum of IR-PEA in $CDCl_3$

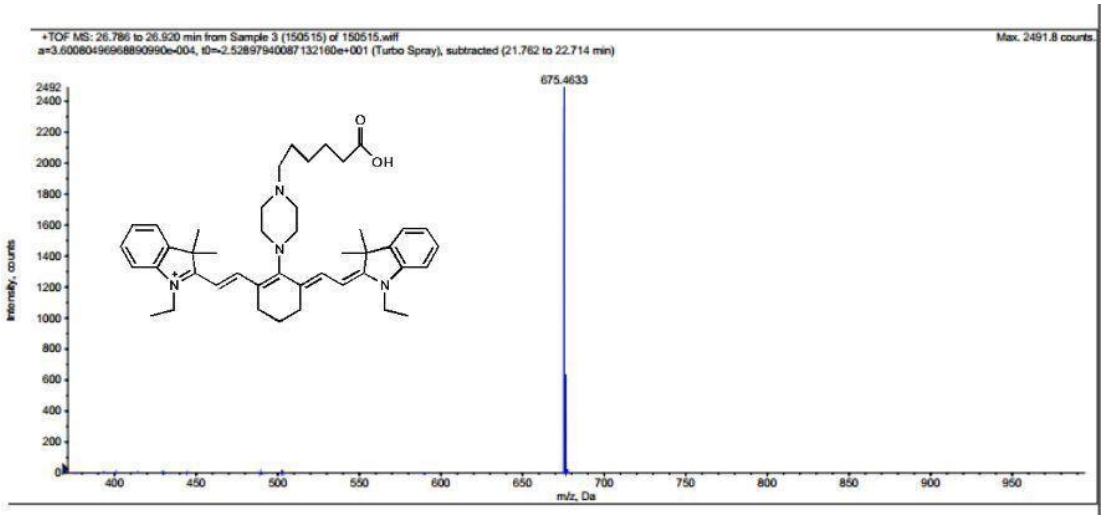

Figure S21. High resolution mass spectrometry (HRMS) of IR-PHA

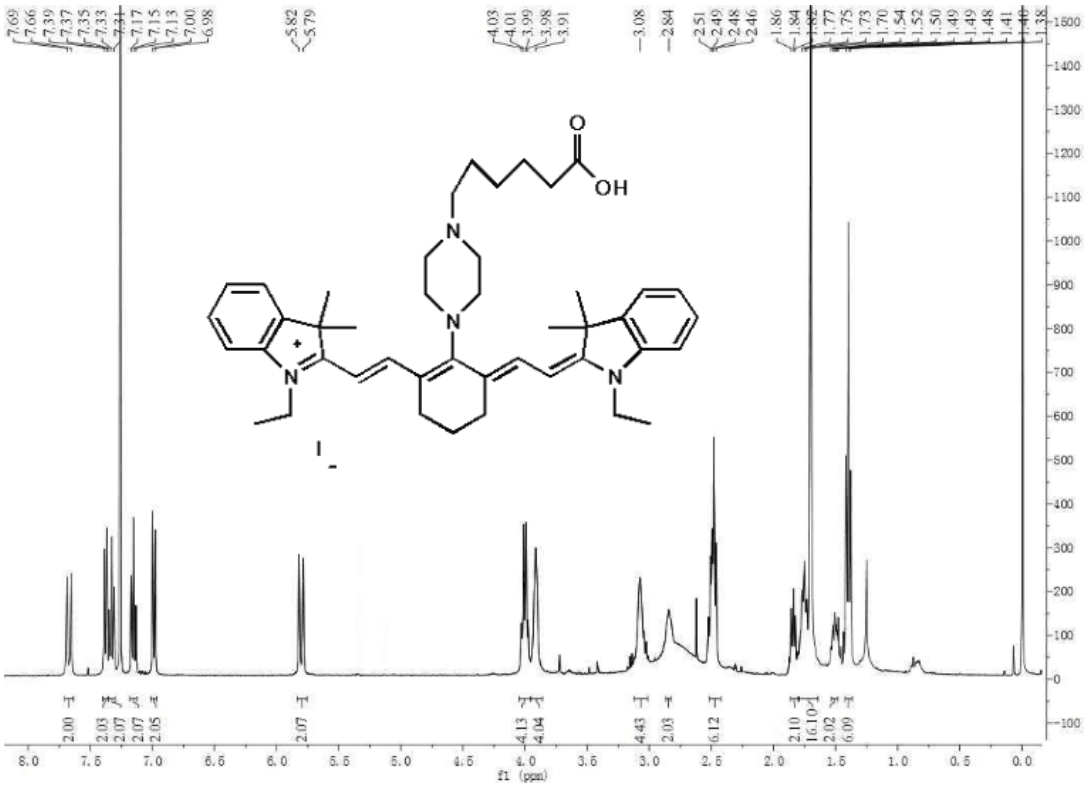

Figure S22. ^{1}H NMR Spectrum of IR-PHA in $CDCl_3$

Table S1. Table S1. The comparison of the developed probe with the published probes.

References	Probes	pH	QY(%)	Abs.(nm)	Em.(nm)	pKa
Anal. Chem. 2015,87, 2495−2503	NIR-Ratio-BTZ	4.0	0.17	608	672	7.2
		8.0	0.21	718	748	
Anal. Chem. 2015,87, 2495−2503	NIR-Ratio-Cl	4.0	0.21	615	677	6.2
		8.0	0.3	698	721	
Anal. Chem. 2015,87, 2495−2503	NER-Ratio-H	4.0	0.28	610	674	7.4
		8.0	0.37	690	708	
Anal. Chem. 2015,87, 2495−2503	NER-Ratio-OMe	4.0	0.24	618	639	6.7
		8.0	0.38	700	720	
Dyes and Pigments 181 (2020) 108611	6a	<7	/	735	815	7.06
		=7	0.128	676	802	
Dyes and Pigments 181 (2020) 108611	6b	<7	/	749	815	6.35
		=7	0.172	677	802	
Dyes and Pigments 181 (2020) 108611	6c	<7	/	663	816	6.08
		=7	0.152	649	803	
Dyes and Pigments 181 (2020) 108611	6d	<7	/	661	804	5.79
		=7	0.104	653	803	
Dyes and Pigments 181	6e	<7	/	658	804	5.13

(2020) 108611		=7	0.156	558	803	
Chem.Sci. 2016,7, 5995–6005	IR1	2.4	0.03	792	778	3.99
		7.4	9.19	712		
Chem.Sci. 2016,7, 5995–6005	IR2	2.4	0.05	774	784	4.56
		7.4	4.63	691		
Chem.Sci. 2016,7, 5995–6005	IR3	2.4	0.05	771	780	4.71
		7.4	6.07	691		
Chem.Sci. 2016,7, 5995–6005	IR4	2.4	0.01	/	783	5.28
		7.4	10.2	677		
Anal. Chem. 2013, 85, 7419−7425	1a	1.6	0.004	666	643	4.5
		9.3	0.01	545	643	
Anal. Chem. 2013, 85, 7419−7425	1b	1.6	0.005	683	720	3.2
		9.3	0.003	565	641	
Anal. Chem. 2013, 85, 7419−7425	3a	1.6	0.01	597	688	2.7
		9.3	0.001	630	723	
Anal. Chem. 2013, 85, 7419−7425	3b	1.6	0.02	663	697	5.8
		9.3	0.001	575	694	
Anal. Chem. 2013, 85, 7419−7425	3c	1.6	0.01	599	694	7.1
		9.3	0.002	593	729	
This work	**IR-PZ**	**<7.4**	**0.03**	**759**	**801**	**7.8**
		>7.4	**0.03**	**679**	**787**	
This work	**IR-PE**	**<6.5**	**0.04**	**761**	**802**	**6.8**
		>6.5	**0.03**	**684**	**784**	
This work	**IR-PZM**	**<4.5**	**0.04**	**767**	**801**	**4.5**
		>4.5	**0.03**	**693**	**787**	
This work	**IR-PEA**	**<3.5**	**0.04**	**762**	**801**	**3.5**
		>3.5	**0.04**	**682**	**784**	
This work	**IR-PHA**	**<6.7**	**0.05**	**759**	**799**	**6.4**

References

(1) Lu, T.; Chen, F. Multiwfn: A Multifunctional Wavefunction Analyzer. J. Comput. Chem.2012, 33, 580- 592.

(2) Humphrey, W.; Dalke, A.; Schulten, K. VMD: Visual Molecular Dynamics. J. Mol.Graphics. 1996, 14, 33-38.